Microstructure and Trapped Magnetic Field of Multi-Seeded Single Domain YBCO

J. Bierlich*, T. Habisreuther, D. Litzkendorf, M. Zeisberger, W. Gawalek

Institute for Physical Hightechnology (IPHT), Jena, Germany

Abstract

The size of the superconducting domains and the critical current density inside these domains have to be enhanced for most of cryomagnetic applications of melt-textured YBCO bulks. To enlarge the size of the domains we studied the multi-seeding technique based on a well-established procedure for preparing high quality YBCO monoliths using self-made SmBCO seeds. The distance between the seeds was optimised as a result of the investigation of the effects of various seed distances on the characteristics of the grain boundary junctions. The influences of a-b plane intersections and c-axis misalignments were researched. Thereby, a small range of tolerance of the misorientations between the seed crystals was found. Field mapping was applied to control the materials quality and the superconductor's grain structure was investigated using polarisation microscopy. YBCO function elements with four seeds in a line and an arrangement of making type (100)/(100) and (110)/(110) boundary junctions, respectively, were processed. The trapped field profile in both sample types shows single domain behaviour. To demonstrate the potential of the multi-seeding method a ring-shaped sample was processed by placing sixteen seeds in a way to make both (100)/(100) and (110)/(110) grain junctions at the same time. The results up to now are very promising to prepare large single domain melt-textured YBCO semi-finished products in complex shapes.

Keywords: Multi-seeded melt-textured YBCO, seed distance, misorientation angle, grain boundaries

I. Introduction

It has been shown that top-seeded melt growth (TSMG) [1], [2] processed $YBa_2Cu_3O_{7-x}$ (YBCO, Y123) superconductors are profitable for most of actual cryomagnetic applications [3]-[6].

At the IPHT in Jena we routinely fabricate YBCO superconductors in batches up to thirty monoliths [3]-[5]. For cylindrical shaped compacts with a diameter up to 60 mm and for samples with a quadratic base up to 60 mm x 60 mm the TSMG takes place by the single-seeding technique [7], [8]. A reproducible manufacture of a large quantity of high-quality single-domain YBCO bulks is guaranteed [3]-[5]. But the size of the Y123 single grain is limited to about 10 cm in diameter [9]-[13] due to the increasing instability of the crystallization front during the melt-texturing [6], [12]. That leads to a degradation of the intragranular electric properties (critical current density, trapped magnetic field) with a larger distance from the

*Corresponding author. Fax: +49 3641 206 199
e-mail: joerg.bierlich@ipht-jena.de

seed and reduced the grain size of high-performance YBCO to about 6 cm, consequently [6], [9]. To overcome this drawback Schätzle et al. [9] developed the multi-seeded melt growth process (MSMG). The MSMG is characterised by a simultaneous growth of single grains from two or more seeds with equal well-defined crystallographic orientations. Consequently, the preparation of massive YBCO semi-finished products in various complex shapes is imaginable.

For the melt crystallisation of rectangular shaped compacts (90 mm x 45 mm x 21 mm) normally we apply a twofold-seeding technique. However, during the MSMG a residual liquid phase and Y_2BaCuO_5 (Y211) particles were pushed by the propagating growth fronts leading to a formation of a non-superconducting grain boundary (GB) [9]-[18].

To enhance the current-carrying capability across GBs and thus to enlarge the size of the superconducting domain we investigated in this study the influences of the seed distance, a-b plane intersections, c-axis misorientations and the GB type on the potential of the multi-seeding technique. The effects of these variables on the trapped magnetic field and the emerged microstructure are reported. Multi seeded quasi-single domain YBCO superconductors will be shown.

II. Experimental

$Y_{1.5}Ba_2Cu_3O_{7-x}$ precursor were pressed to form both cylindrical compacts with diameters of 35 mm as well 60 mm and 19 mm in height and cuboids with a dimension of 42 mm x 42 mm x 21 mm. Further details on the sample preparation and the heat treatment can be found elsewhere [3]. The sample seeding takes place on the basis of self-made $SmBa_2Cu_3O_{7-x}$ seeds with dimensions of about 2 mm x 2 mm x 2 mm. Particulars of the efficient fabrication of the seeds are still published [19]. Before seeding the compacts the cleaved a-b contact surface of the seeds was observed with polarized optical microscopy to ensure its single grain character

and ascertain the crystal orientation. Different numbers of seeds (two to sixteen) were arranged of making (100)/(100) and (110)/(110) GB junctions. To investigate the influence of the seed distance variably mutual distances (d_1) between 2 mm and 20 mm were tested. Note, that the seed distance is shortened by about 15% due to the sample shrinkage while the heat treatment. Seed distances before processing are denoted by d_1 and after that by d_2. The influence of the a-b plane intersection angle (θ) and the angle of c-axis misalignments (ψ) were studied by means of provoked misorientations in the range of 0° to 15°. For the preparation of large YBCO superconductors a constant seed distance of $d_1=5$ mm was applied. The trapped magnetic field profile was detected by scanning the sample surface with a hall sensor at a distance of 0.6 mm at 77 K [5], [20]. The microstructure was inspected through polarized optical microscopy.

III. Influence of the seed distance

Twofold seeded YBCO samples ($\varnothing=35$ mm) were grown with different seed distances and a seed arrangement to form both (100)/(100) and
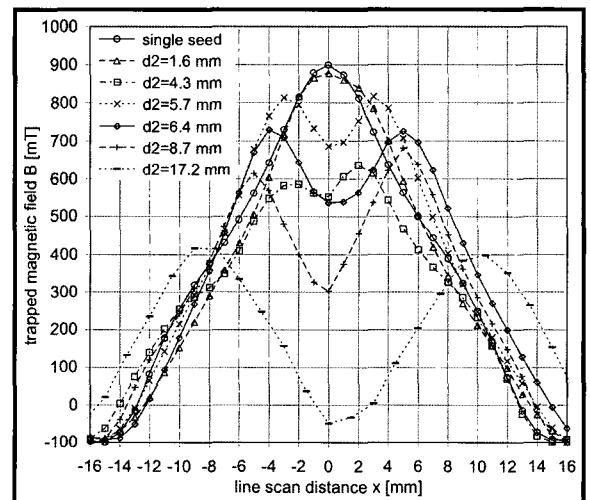

Fig. 1. Trapped magnetic field distributions crossing the (100)/(100) grain boundary along the seeds in comparison with the field distribution measured in a single seed sample.
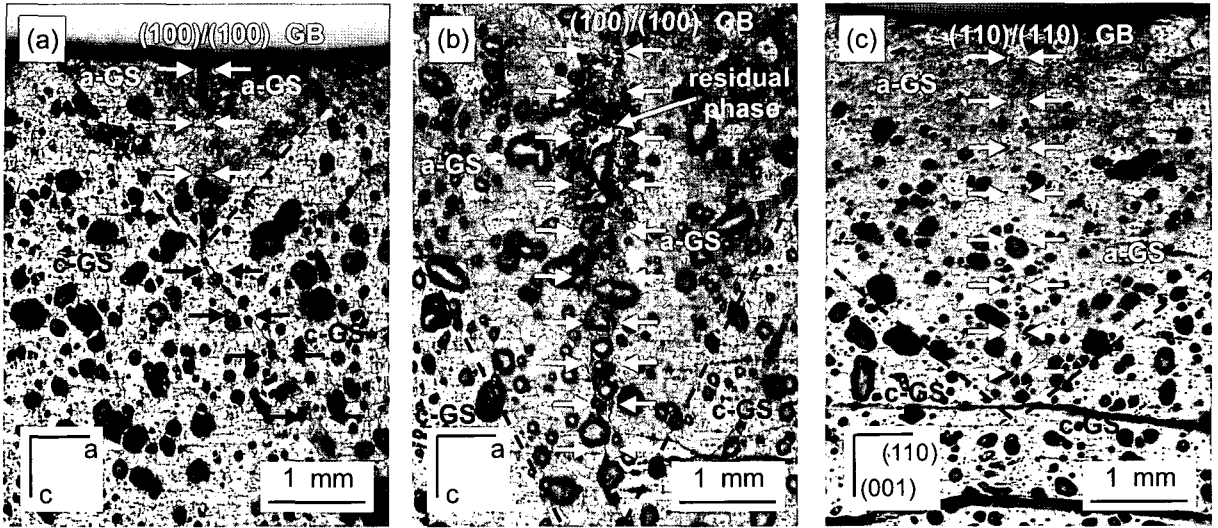
Fig. 2. Microstructure in the a-c cross section, observed in samples with (a) a seed distance d_2=1.6 mm and (b) d_2=8.7 mm around (100)/(100) GBs as well as (c) d_2=8.8 mm around a (110)/(110) GB.

(110)/(110) GBs. All samples showed two undisturbed Y123 grains grown from equivalent seeds. Fig. 1 represents the trapped magnetic field distribution of the (100)/(100) samples crossing the GBs along the seeds in comparison with the field distribution obtained from a single-seed sample. The sample with d_2=1.6 mm shows just like the single-seeded sample a single domain field profile. The result indicates an unresisted current transport capability across this GB and thus a grain junction of very high quality. However, for d_2>1.6 mm a depression of the magnetic flux density is observed. The connectivity at the GB is distinctly decreasing as the seed distances increased and even drops to zero at d_2=17.2 mm. This effect is in accordance with the increasing of the non-superconducting segregation layer at the GBs in the a-growth sectors (a-GS) as the seed distance becomes larger [10]-[12].

Fig. 2 shows the microstructure in the a-c cross section, observed in samples with (a) d_2=1.6 mm and (b) d_2=8.7 mm around (100)/(100) GBs as well as (c) d_2=8.8 mm around a (110)/(110) GB. In the former case it can been seen that with larger seed distances an increasing amount of residual phase (CuO, $BaCuO_2$ and Y211) is accumulate in front of the

(100) growth facets due to the larger range for the growing Y123 grains to impinge each other. Therefore, in the sample with d_2=1.6 mm the GB (white arrows) is very clean and the conically shaped region (black dashed lines) where the GB is composed of a-GSs is smaller compared to the other [18]. In the c-growth sectors (c-GS) the (001) growth fronts push the impurity phase towards the sample bottom resulting in a relatively secondary phase clean GB (black arrows) [12], [18].

Fig. 3 represents the ratio of the lowest trapped magnetic field value at the GB (deflection between the peaks) to the averaged maximum field in dependence on the seed distance (d_2) for both GB types. The (110)/(110) GBs show a lower reduction of the magnetic flux density with increasing seed distances than the (100)/(100) GBs. In comparison with the microstructure of the (100) type GB (d_2=8.7 mm) (Fig. 2(b)) the (110) GB (d_2=8.8 mm) (Fig. 2(c)) in a-GS and c-GS, respectively, are observed to be associated with relatively clean grain junctions (white arrows) [14]-[18]. In the vicinity of the seeds, the conically shaped a-GS region (black dashed lines) is fewer expanded into the sample volume than in the (100) GB samples. This is because, the growth rate in [110] direction is as
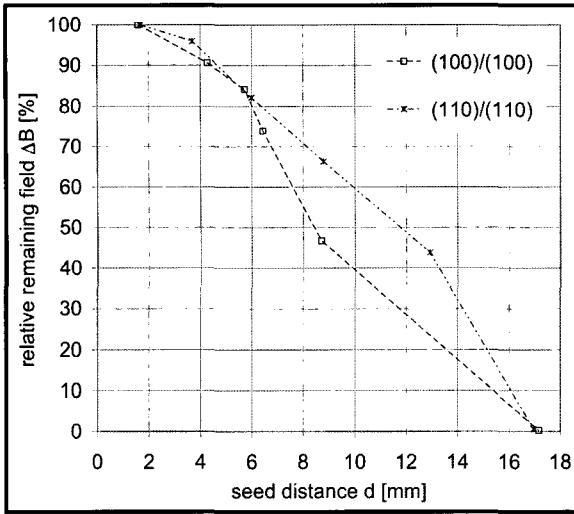
Fig. 3. The ratio of the strongest trapped magnetic field deflection between the maximum points to the averaged maximum field in dependence on the seed distance at both (100)/(100) and (110)/(110) grain boundaries.

faster as in [100] direction and therefore the {100} growth facets of Y123 grains take a longer period until they impinge each other [4], [9]. However, the two-dimensional flux distribution of a (110)/(110) sample shows a lateral contraction of the trapped field along the GB (Fig. 4(a)). The whole (110)/(110) GB were formed by impingement of {110} growth facets leading to an increasing accumulation of

insulating phases towards the sample outside. Fig. 4(b) shows by contrast an equal distribution of the flux density along the (100)/(100) GB. That GB type consists of a stronger contaminated section in the space between the seeds and a remaining nearly impurity free region.

In principle both grain boundary types are useful to achieve strongly coupled grain junctions. For the preparation of function elements we decided a seeding with $d_1=5$ mm. An adequate connectivity of the Y123 grains as well to minimise the number of GBs per bulk are the reasons for that decision.

IV. Influence of misorientations

It is known that the intergranular current density is very sensitive to misorientations of two adjacent grains. However, the published values of e.g. the a-b plane intersection angle (θ) acts as weak link scatters for YBCO from $\theta>3°$ to $\theta>15°$ [16]-[18]. This may be because the nonuniform production conditions.

To find out tolerable misorientations under our fabrication conditions double seeded samples ($\varnothing=35$ mm) were prepared applying a constant seed distance of $d_1=7$ mm and an arrangement of making defined misoriented (100)/(100) GB junctions. For these purposes we investigated on
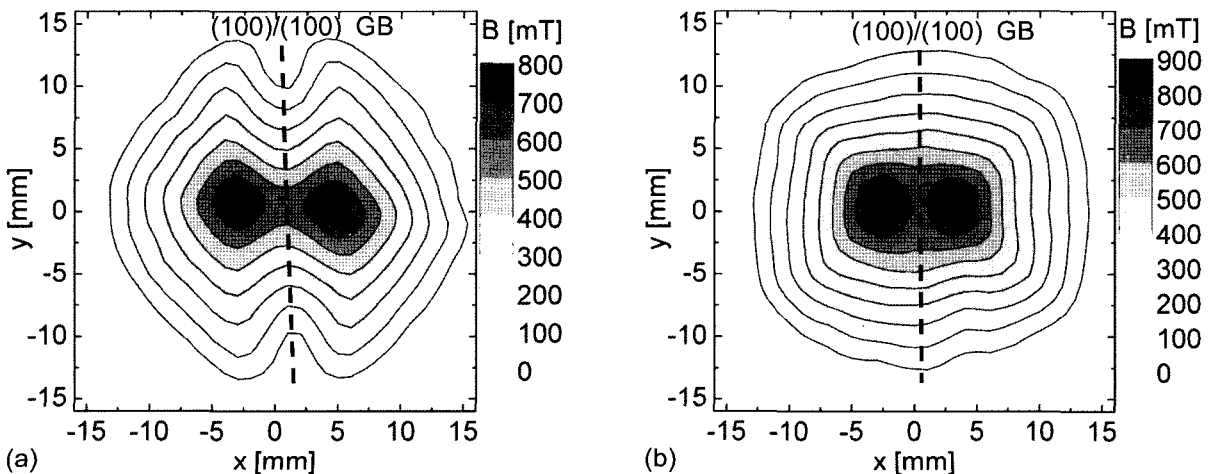

(a)

(b)

Fig. 4. The two-dimensional flux distribution of (a) a (110)/(110) grain boundary sample and (b) a (100)/(100) grain boundary sample.
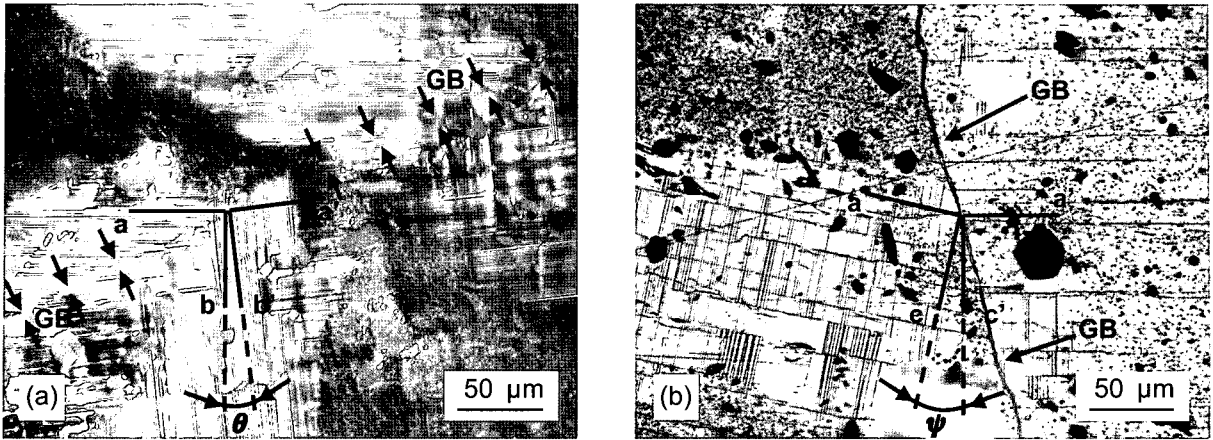
Fig. 5. The microstructure around the grain boundary of misoriented samples shows (a) a-b planes twisted by θ=6° and (b) c-axes misaligned by ψ=14°.

separate samples the influence of both a-b plane intersection angles (θ) and c-axis misalignments (ψ) in the range of 0° to 15°. To control the deviations of the Y123 grains the crystallographic orientation of the seeds was preset and the emerged microstructure of the processed samples was checked by polarization microscopy. The degree of the misorientations was ascertained on the basis of the direction of the twin patterns and a-b macrocracks [21], respectively. As an example illustrated in Fig. 5(a) the microstructure of a-b planes around the GB (black arrows) of two adjacent grains twisted by θ=6°. Fig. 5(b) shows the a-c cross section of two grains observed in a sample with a misalignment caused by a declination of the grain's c-axes by ψ=14°.

In Fig. 6 is shown the ratio of the magnetic field deflection at the GBs to the averaged maximum field in dependence on the tested misorientation angles. The results indicate a rapidly increasing depression of the connectivity at the grain junctions with an increasing a-b plane intersection angle as well as an increasing angle of c-axis misalignments. The well-oriented sample with θ=0° and ψ=0° acts as reference. In that case the deterioration of the trapped field of about 26% of the maximum field is presumably ascribable to the seed distance. The tested misorientation angles up to 10° are in the same range like low-angle boundaries between

subgrains. However, low-angle boundaries were believed not to act as weak links [22]. In contrast the strong reduction of the current transport capability at the GB in that study takes place for θ>2° and ψ>5°, respectively. Here the width of the GB becomes important because of the limited coherent length that makes the GB weak link. All these leads to a small range of tolerance while the seeding of more numerous seeds for the production of large YBCO monoliths in complex shapes.
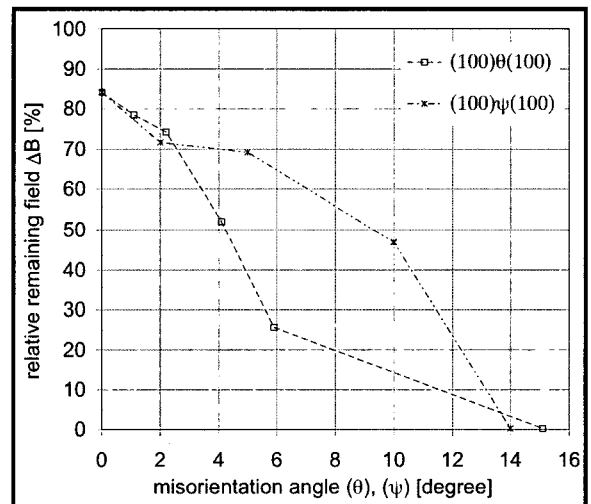

Fig. 6. The ratio of the magnetic field deflection at the GBs to the averaged maximum field in dependence on the tested a-b plane intersection angles (θ) and c-axis misalignments (ψ).

V. YBCO function elements

To scale up the sample size by MSMG further growth experiments was made. Fourfold in-line seeded compacts (42 mm x 42 mm x 21 mm) with arrangements of forming (100)/(100) and (110)/(110) GBs, respectively, were processed. The distance between the seeds was defined to be d_1=5 mm. Fig. 7(a) shows the top view of a sample consisting of four Y123 single grains coupled by three (100)/(100) GBs. In another sample (Fig. 7(b)) the crystallographic orientation of the seeds in the a-b planes was turned by 45° so that (110)/(110) GBs were formed. Although these samples consist of several single grains the trapped field distribution in both cases reveals magnetic single domain behaviour. The reached maximum value of the trapped magnetic field is 918 mT for the (100) type sample (Fig. 7(c)) and 973 mT for the (110) type sample (Fig. 7(d)), respectively.

A function element for applying as secondary winding of an inductive fault current limiter (FCL)
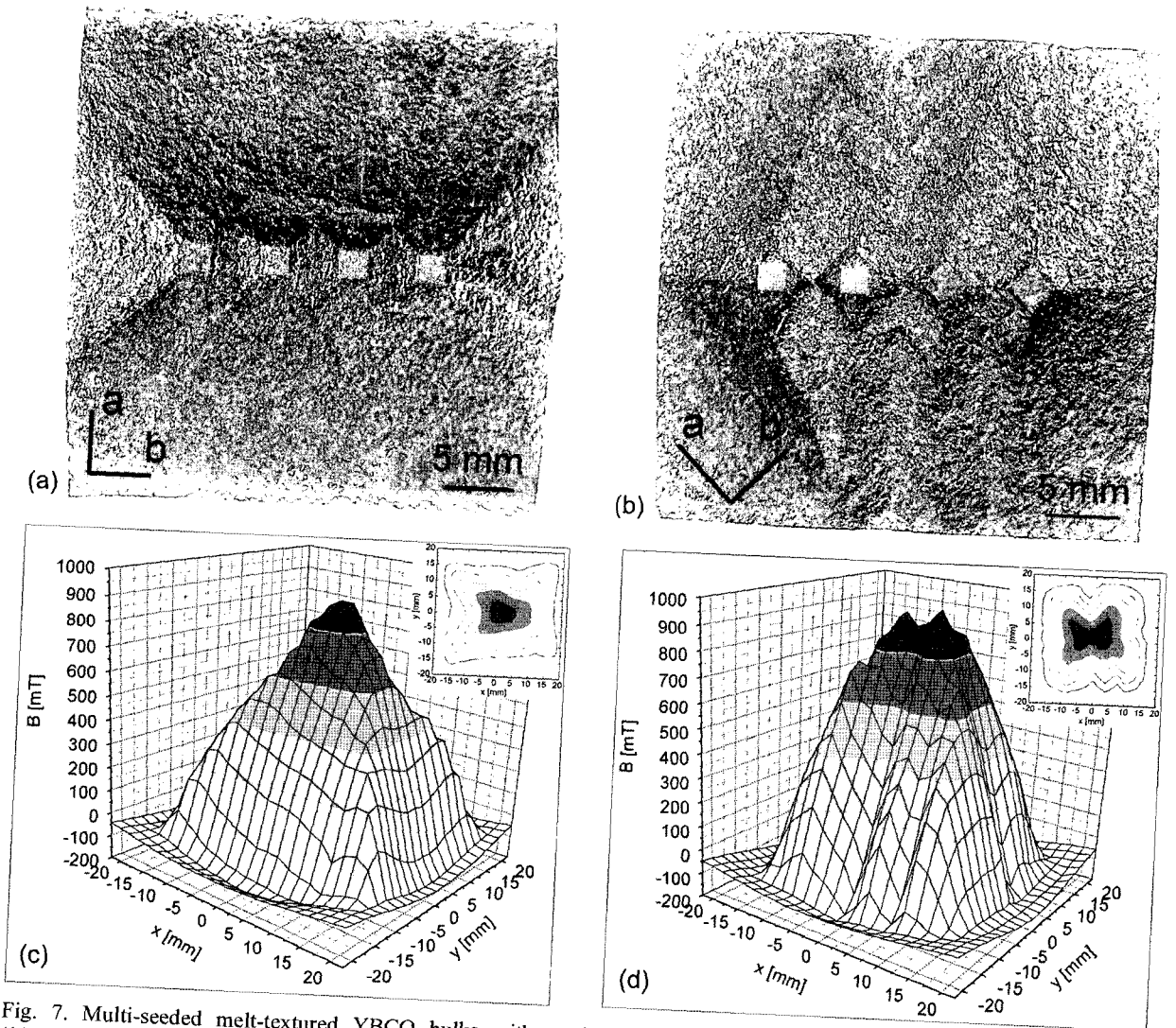

Fig. 7. Multi-seeded melt-textured YBCO bulks with seed arrangements of growing both (a) (100)/(100) and (b) (110)/(110) grain boundary junctions as well as the trapped field distribution of these monoliths for (c) the (100) type sample and (d) the (110) type sample.
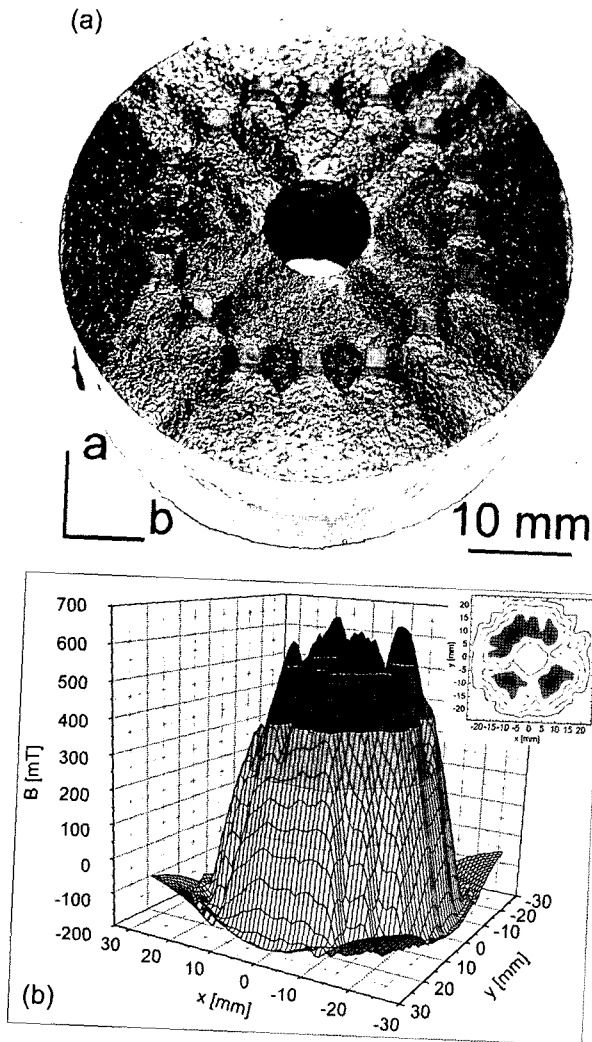
(a)

(b)

Fig. 8. Ring-shaped YBCO bulk superconductor (a), melt-processed by placing sixteen seeds in a way to make both (100)/(100) and (110)/(110) GBs as well as (b) trapped field distribution of that sample at 77 K.

to each other. That is basically caused by the shrinkage of the compacts during the sintering stage and the melt processing [14], [16]. The obtained misaligned GBs result in a degradation of the current transport capability as has been already described in passage IV. Therefore, the sample shows multi peaks around the inner hole. However, a homogenous field of 300 mT was trapped above the hole indicating a superconducting transport current across all sixteen grains junctions. Thus, that sample acts similar like an air-core cylindrical inductor.

VI. Conclusions

To enlarge the domain size in YBCO bulk superconductors we investigated the multi-seeding technique using melt-textured Sm123 as heterogeneous seeds. The distance between the seeds was optimised considering of an adequate current transport capability across grain boundaries. It was shown, that the trapped field distribution in a multi-grain sample is strong dependent on grain's misorientation. Thus, the orientation of the seeds has to adjust within a small range of tolerance. Large single domain samples were achieved at a seed distance of 5 mm. Both (100)/(100) and (110)/(110) grain junction types are applicable even simultaneously at the same sample. Further investigations and more complex growth experiments are necessary to assure the multi-seeding technology. An important point is the avoidance of the seed displacement due to sample shrinkage. We suggest at first to sinter the compacts and afterwards to place the seeds at the cold sintered body. The results up to now are very promising to prepare large near-net shaped single domain YBCO bulk superconductors.

[23] shows Fig. 8(a). The illustrated ring-shaped sample ($\varnothing_{outer}$=52 mm, $\varnothing_{inner}$=12 mm, h=18 mm) was processed by placing sixteen seeds in a way to make both (100)/(100) and (110)/(110) GBs at the same time. A seed distance of d_1=5 mm was applied.

In the field profile (Fig. 8(b)) several peaks and deteriorations are observed, which correspond to the grain centres and the weakly linked grain junctions. Although the seed distance and the orientation of the seeds were controlled the location of several seeds after processing was slightly misoriented with respect

Steinmetz, M. Arnz and B. Borns for technical support.

References

[1] Morita M, Takebayashi S, Tanaka M, Kimura K, Miyamoto K and Sawano K 1991 *Adv. Supercond.* 3 733

[2] Lo W, Cardwell D A, Dewhurst C D and Dung S-L 1996 *J. Mater. Res.* 11 786

[3] Litzkendorf D, Habisreuther T, Bierlich J, Surzhenko O, Zeisberger M, Kracunovska S and Gawalek W 2005 *Supercond. Sci. Technol.* 18 S206-208

[4] Habisreuther T, Zeisberger M, Litzkendorf D, Surzhenko O, Kracunovska S, Bierlich J, Kosa J, Vajda I and Gawalek W 2004 *Progress in Superconductivity* Vol.6 No.1 pp1-6

[5] Habisreuther T, Litzkendorf D, Prikhna T A, Müller R, Zeisberger M, Kracunovska S, Bierlich J and Gawalek W 2003 *Ceramic Transactions* No.140 pp337-350

[6] Hull J R and Murakami M 2004 *Proceedings of the IEEE* Vol.92, No.10 pp.1705-1718

[7] Salama K and Lee D F 1993 *Appl. Supercond.* 261-268

[8] Jee Y A, Hong G-W and Kim C-J 1999 *IEEE Trans. Appl. Supercond.* 9 2097-2100

[9] Schätzle P, Krabbes G, Stöver G, Fuchs G and Schläfer D 1999 *Supercond. Sci. Technol.* 12 S69-76

[10] Jee Y A, Kim C-J, Sung T-H and Hong G-W 2000 *Supercond. Sci. Technol.* 13 S195-201

[11] Kim C-J, Kim H-J, Joo J-H, Hong G-W, Han S-C, Han Y-H, Sung T-H and Kim S-J 2000 *Physica C* 336 233

[12] Jooss Ch, Bringman B, Delamare M P, Walter H, Leenders A and Freyhardt H C 2001 *Supercond. Sci. Technol.* 14 S260-275

[13] Sawamura M, Morita M and Hirano H 2004 *Supercond. Sci. Technol.* 17 S418-421

[14] Kim C-J, Kim H-J, Jee Y A, Hong G-W, Joo J-H, Han S-C, Han Y-H, Sung T-H and Kim S-J 2000 *Physica C* 338 205

[15] Kim H-J, Kim C-J, Hong G-W and Joo J-H 2002 *Physica C* 372-376 1159

[16] Furusawa K, Chikumoto N, Ogasawara K, Nagatomo T and Murakami M 2002 *Physica C* 378-381 255

[17] Reddy E S, Noudem J G, Tarka M, Noe M and Schmitz G J 2002 *Supercond. Sci. Technol.* 15 S48-53

[18] Delamare M P, Bringmann B, Jooss Ch, Walter H, Leenders A and Freyhardt H C 2002 *Supercond. Sci. Technol.* 15 S16-22

[19] Bierlich J, Habisreuther T, Litzkendorf D, Dubs C, Müller R, Kracunovska S and Gawalek W 2005 *Supercond. Sci. Technol.* 18 S194-197

[20] Zeisberger M, Habisreuther T, Litzkendorf D, Müller R, Surzhenko O and Gawalek W 2002 *Physica C* 372-376 1890

[21] Kracunovska S, Diko P, Litzkendorf D, Habisreuther T, Bierlich J and Gawalek 2005 *Supercond. Sci. Technol.* 18 S142-148

[22] Diko P 2000 *Supercond. Sci. Technol.* 13 S1202-1213

[23] Györe A, Farkas L and Vajda I 2005 *Supercond. Sci. Technol.* 18 S82-85